Classification

Biological Sciences, Microbiology

Title

Dendritic transport of tick-borne flavivirus RNA by neuronal granule affects development of the neurological disease.

Short title

Hijacking of mRNA transport in dendrites by TBEV

Authors

Minato Hirano, Memi Muto, Mizuki Sakai, Hirofumi Kondo, Shintaro Kobayashi, Hiroaki Kariwa and Kentaro Yoshii *

Laboratory of Public Health, Faculty of Veterinary Medicine, Hokkaido University

*Corresponding author
Kentaro Yoshii, PhD., DVM.
Laboratory of Public Health, Faculty of Veterinary Medicine, Hokkaido University,
kita-18 nishi-9, kita-ku, Sapporo, Hokkaido 060-0818, Japan
Tel/fax: +81-11-706-5212
E-mail: kyoshii@vetmed.hokudai.ac.jp

Author contributions

Conceived and designed the experiments: K.Y. and M.H. Performed the experiments: M.H., M.M., M.S., H.Kondo, S.K. and K.Y. Analyzed the data: M.H., M.M., and S.K. Wrote the paper: M.H., S.K., H. Kariwa and K.Y. All authors reviewed the manuscript.

Keywords

Tick-borne encephalitis virus, Flavivirus, Neuropathogenicity, Neuronal granule, Dendritic mRNA

Abstract

Neurological diseases caused by encephalitic flaviviruses are severe and associated with high levels of mortality. However, little is known about the detailed mechanisms of viral replication and pathogenicity in the brain. Previously, we reported that the genomic RNA of tick-borne encephalitis virus (TBEV), a member of genus *Flavivirus*, is transported and replicated in the dendrites of neurons. In the present study, we analyzed the transport mechanism of the viral genome to dendrites. We identified specific sequences of the 5′ untranslated region of TBEV genomic RNA that act as a *cis*-acting element for RNA transport. Mutated TBEV with impaired RNA transport in dendrites caused a reduction in neurological symptoms in infected mice. We showed that neuronal granules, which regulate the transport and local translation of dendritic mRNAs, are involved in TBEV genomic RNA transport. TBEV genomic RNA bound a RNA-binding protein of neuronal granules and disturbed the transport of dendritic mRNAs. This is the first report of a neuropathogenic virus hijacking the neuronal granule system for the transport of viral genomic RNA in dendrites, resulting in severe neurological disease.

Significance statement

Flaviviruses represent a significant threat to public health worldwide, and several flaviviruses cause severe neurological disease in humans and animals. However, no specific treatment has been developed due to the lack of information about the detailed pathogenic mechanisms. In current study, we revealed that the transport of the viral RNA of tick-borne flavivirus in neuronal dendrites was involved in the development of the neurological disease. The virus hijacked the transport system of host mRNA in dendrites, which is important for neuronal functions, such as neurogenesis and the plasticity of the synaptic communication. Our findings of this unique virus-host interaction will promote the study of neurodegenerative diseases caused by disruption of dendritic mRNA transport and development of their treatment.

¥body

Introduction

Flavivirus is a genus in the family *Flaviviridae* and has a single-stranded RNA with positive polarity serving as an mRNA for translation (1). The genome encodes one polyprotein, which is post-translationally cleaved into three structural and seven non-structural (NS) proteins, within a single long coding sequence (CDS). The structural and NS proteins form a virus particle and a viral replication complex, respectively. The 5′ and 3′ untranslated regions (UTRs) are involved in the stability, translation, and replication of the genomic RNA (2, 3). The genus *Flavivirus* contains more than 70 members, many of which are arthropod-borne pathogens distributed all over the world (4). Many outbreaks have been reported, and flaviviruses have been attracting global attention as emerging or re-emerging infectious diseases (5, 6).

Some of the pathogenic flaviviruses, such as Japanese encephalitis virus, West Nile virus (WNV), and tick-borne encephalitis virus (TBEV), are neurotropic and cause encephalitic disease (4). The encephalitic flaviviruses histologically induce typical nonsuppurative encephalitis (4, 7). However, differences in neurological symptoms were observed in the flaviviruses, and neurologic manifestations such as photophobia, irritability, and sleep disorders are characteristically observed following TBEV infection (8, 9). These differences in the symptoms have suggested that the pathogenic mechanism in neurons may differ in the encephalitic flaviviruses. Previously, we reported that the genomic RNA of TBEV was specifically transported from the cell body to dendrites and replicated locally in dendrites in primary cultures of mouse neurons (10). Genomic RNA transport and local replication are thought to be important in the pathogenesis of neurological diseases that are result of TBEV infection, although their detailed mechanism are not well understood.

It has been reported that mRNAs are transported and locally translated in neuronal dendrites (11). Specific mRNAs form a complex, called a neuronal granule, with several RNA-binding proteins (RBPs), and are transported along microtubules to dendrites in a kinesin-dependent manner. Transport of the mRNA and local translation in neuronal dendrites have been shown to be important for neurogenesis and the plasticity of the synaptic communication (12, 13). Furthermore, disruption of the neuronal granule system has been shown to be involved in mental retardation and neurodegenerative diseases, such as fragile X syndrome (14), autism

spectrum disorder (15), and Alzheimer's disease (16). We hypothesized that the genomic RNA of TBEV is also transported by neuronal granules, resulting in the severe neurological symptoms caused by TBEV infection.

In this study, we investigated the mechanism of the transport of TBEV genomic RNA transport to the dendrites in neurons. We identified a *cis*-acting element in the viral genomic RNA important for transport. Genomic RNA transport contributed to the development of neurological symptoms following TBEV infection. TBEV genomic RNA interacted with an RBP of neuronal granules and disturbed the transport dendritic mRNAs using neuronal granules for dendritic transport.

Results

1. 5′ UTR of TBEV is a cis*-acting element important for RNA transport to neurites.*

PC12 cells differentiate into neuronal phenotype and form neurites in the presence of neuronal growth factors. To examine whether the genomic RNA of TBEV is transported to neurites in differentiated PC12 cells, as observed in primary neurons (10, 17), the PC12 cells were infected with TBEV. Accumulations of viral antigen and fluorescent in-situ hybridization (FISH) signal for TBEV genomic RNA were observed in the neurites (Fig. S1), as seen in the dendrites of the primary neurons.

To analyze the RNA region required for transport, plasmids expressing RNA for a luciferase CDS fused with partial sequences of the TBEV were constructed (Fig. 1A). Expressed RNA with TBEV UTRs was detected in neurites, but those with any of the CDS for the viral proteins were not (Fig. 1B and C), indicating that the UTRs of TBEV, but not viral proteins, were important for the transport of mRNA to neurites.

In our previous study, we observed the viral antigen accumulations in dendrites of cells infected with tick-borne flaviviruses, but not in those infected with mosquito-borne WNV (10). We hypothesized that this difference could be caused by differences in the UTRs and constructed plasmids expressing luciferase mRNA with the UTRs of TBEV or WNV (Fig. 1D). The mRNAs expressed with the 5′ UTR of TBEV were localized to neurites, while those with the 5′ UTR of WNV were not, regardless of the 3′ UTR sequences (Fig. 1E and F). Complete deletion of the 3′ UTR drastically reduced the expression of the RNAs in reporter assay,

indicating that the 3′ UTR was involved in the stability of the RNAs (Fig. S2A). These data suggest that the 5′ UTR of TBEV contains a motif required for the transport of mRNA to neurites.

There are two stem-loop (SL) structures (SL-1, nucleotide (nt) 4–103 and SL-2, nt 107–128) predicted in the 5′ UTR of TBEV (18) (Figs. 2A and S3). A plasmid with deletion of SL-1 or SL-2 in the 5′ UTR was constructed to analyze the importance of these structures in transport (Fig. 2A). The mRNA with deletion of SL-1 was still detected in the neurites, while deletion of SL-2 abolished the localization (Fig. 2B and C). These data indicated that the SL-2 region of TBEV 5′ UTR is required for mRNA transport.

To further analyze the role of SL-2, we introduced mutations in the SL-2 region of pCMV-Luc (5′ TBEV/3′ TBEV). The mutations of SL-2 loop G-U and C-U were designed without affecting formation of the stem structure. The mutations of SL-2 stem were designed to dissociate the stem structure (Fig. 2D). After transfection of PC12 cells, the mutation of SL-2 loop G-U or SL-2 stem slightly decreased the signals in the neurites. However, the mRNAs with the mutation was still detected in the neurites, and showed no significant difference from those of TBEV wild-type (wt). The mRNAs with the SL-2 loop C-U mutation were not detected in the neurites completely (Fig. 2E and F). These indicated that C at nt position 120 in SL-2 is the most important in the transport of mRNA to neurites.

2. Mutation-impeding genome transport to dendrites attenuated the neurological symptom of TBEV

To construct a mutant TBEV lacking the ability to transport the genome in dendrites, a C-to-U mutation at nt position 120 in the 5′ UTR was introduced into the infectious clone of TBEV. The recovered mutant virus (SL-2 loop C-U) grew relatively slower until 24 h post-infection (h.p.i.), but caught up with that of TBEV wt by 48 h.p.i. in primary cultures of mouse neurons (Fig. S4). Viral genomic RNA was detected in the dendrites infected with TBEV wt, but the signal in dendrites was weak in SL-2 loop C-U-infected cells (Fig. 3A). Number of the viral antigen accumulation in the dendrites also decreased significantly in cells infected with SL-2 loop C-U (Fig. 3A and B), indicating that the C-U mutation of the SL-2 loop significantly decreased the transport of genomic RNA to dendrites.

To evaluate the effects of TBEV genome transport on the pathogenesis in mice, C57BL/6 mice were

135 inoculated with TBEV wt or SL-2 loop C-U intracerebrally. No differences in morbidity or mortality were
136 observed between the two groups (Fig. 3C). Slightly prolonged survival time (TBEV wt, 7.9 ± 0.46 d
137 post-infection (d.p.i.); SL-2 loop C-U, 8.9 ± 0.68 d.p.i.; $p < 0.02$) were observed in the mice infected with
138 SL-2 loop C-U. The number of mice showing severe neurological symptoms was reduced (TBEV wt, 70%;
139 SL-2 loop C-U, 30%), and the level of cerebellar ataxia of infected mice was scored and was found to be
140 significantly lower from 5 to 7 d.p.i. in mice infected with SL-2 loop C-U (Fig. 3D). The virus titer was lower
141 in the brain infected with SL-2 loop C-U at 3 d.p.i., but caught up with TBEV wt at 6 d.p.i. (Fig. 3E). No
142 reversion or compensatory mutation in the 5′ UTR was found in the mice infected with SL-2 loop C-U. Thus,
143 preventing the transport of the genome did not affect the lethality after viral multiplication, but attenuated the
144 neurological symptoms of TBEV in mice.
145
146 *3. Role of neuronal granules in viral genome transport*
147 Neuronal granules have been shown to regulate the transport of mRNAs and local protein translation in
148 neuronal dendrites (11). We hypothesized that neuronal granules are involved in the transport of TBEV
149 genomic RNA and local viral replication. Colocalization of viral proteins and RNA to RBPs in neuronal
150 granules, such as, fragile X mental retardation protein (FMRP), RNA granule protein 105 (RNG105), and
151 Staufen, was analyzed in primary neurons infected with TBEV wt or SL-2 loop C-U. Viral antigen
152 accumulation, viral RNA and the RBPs were detected in the same neurites infected with TBEV wt (Figs. 4, S5
153 and S6), suggesting that TBEV genomic RNA was transported via the neuronal granule. However, their
154 detailed localizations varied. FMRP colocalized with viral antigen and was recruited into the site of the viral
155 antigen in the dendrites. Signals of FMRP in the neurites increased significantly in the neuron infected with
156 TBEV wt (Figs. 4 and S5). In contrast, RNG105 surrounded the accumulation of viral antigen, but did not
157 completely colocalize with the viral protein. (Figs. 4 and S5).
158 To further analyze the interaction of the neuronal granule RBPs and viral genomic RNA, binding of
159 FMRP to the genomic RNA of TBEV was examined. *In vitro* synthesized RNAs of the full-length TBEV
160 genome were mixed with Flag-tagged FMRP expressed in human embryonic kidney cells 293T. RNAs that

coimmunoprecipitated with FMRP were detected by reverse transcription (RT-) PCR. RNAs for TBEV wt coimmunoprecipitated with FMRP, while RNAs with C-to-U mutation at nt 120 in the SL-2 region showed decreased binding (Fig. 5A). A missense mutation (I304N) was identified in the second K homology domain of the *FMRP* gene of a fragile X syndrome patient and shown to be involved in altered RNA binding and transport (19, 20). This mutation was found to drastically reduce the binding of FMRP to TBEV genomic RNA (Fig. 5B). These results indicated that SL-2 region of TBEV 5′ UTR, important for the transport, is also critical for binding to an RBP of neuronal granule, FMRP. It was also shown that the transported TBEV genomic RNA altered the distribution of bound FMRP in neuronal granules.

To evaluate the effect of TBEV genome transport on neuronal function, the distribution and expression of host mRNAs for Arc, brain-derived neurotrophic factor (BDNF), and Ca^{2+}/calmodulin-dependent protein kinase II α (CaMKIIα) were examined in primary neurons infected with TBEV wt or SL-2 loop C-U. The mRNA signals in dendrites, especially the mRNA of BDNF, decreased significantly in neurons infected with TBEV wt but not in those infected with SL-2 loop C-U (Fig. 6). The expression of the mRNAs was reduced more by infection of TBEV wt than SL-2 Loop C-U (Fig. S7). These results indicate that the transport of TBEV genomic RNA disturbed that of host dendritic mRNAs.

Discussion

The transport of TBEV genomic RNA occurred independently of viral proteins and differed from that of other neurotropic viruses. Dendritic and axonal transport of viral genomes has been reported in several neurotropic DNA and RNA viruses (21). The genomic DNA of herpes simplex virus type 1 and 2 (*Herpesviridae*) undergo anterograde or retrograde transport through the binding of viral proteins with host motor proteins (22). Virions of poliovirus (*Picornaviridae*) are known to be incorporated into synaptic vesicles during anterograde transport (23). Complexes of nucleoprotein and genomic RNA of rabies virus (*Rhabdoviridae*) are transferred via retrograde processes (24). The genomes of these viruses require their viral proteins for transport, while our data showed that the transport of TBEV genomic RNA in dendrites occurs independently of the viral proteins and is regulated by the UTR of the genomic RNA itself (Figs. 1 and 2).

187 Besides, the viral genome of reported neurotropic viruses usually replicated in the neuronal cell body.
188 However, transported TBEV genomes replicate locally in the dendrites, which has not been reported in other
189 neurotropic viruses.

190 The 5′ UTR of TBEV was demonstrated to have a function in RNA transport, in addition to protein
191 translation and genome replication. The UTRs of flavivirus are important for many functions in viral
192 multiplication. The complementary sequences in the 5′ and 3′ UTRs cyclize the viral genome, which is
193 essential for viral genome replication (2, 3, 18). SL-1 in the 5′ UTR is thought to recruit the nonstructural
194 protein 5 (NS5) protein for genome replication (3, 25). The loop C-U mutation introduced to the recombinant
195 TBEV overlapped with the cyclization sequences and therefore may affect genome cyclization, resulting in
196 delayed viral growth and decreased neurological symptoms (Figs. 3D, 3E and S4). However, RNA with the
197 TBEV 5′ UTR and WNV 3′ UTR, which could not cyclize the RNA, was efficiently transported to the neurite,
198 indicating that transport was independent of the TBEV 3′ UTR and genome cyclization (Fig. 1D–F). In
199 addition, reporter assay revealed that, regardless of the transport of the genome, the mutations introduced to 5′
200 UTR did not affect RNA stability or translation efficiency, but the deletion of 3′ UTR drastically reduced the
201 stability (Fig. S2). These results suggest that genome transport via the SL-2 region is independent of other
202 known functions of 5′ UTR, and that the TBEV 3′ UTR was not directly involved in the transport although it
203 stabilized the RNA.

204 SL-2 in the 5′ UTR of TBEV genomic RNA was shown to be a unique viral *cis*-acting element
205 important for the transport of mRNA. Mutant RNA that cannot form the stem structure (SL-2 stem) was still
206 transported to dendrites (Fig. 2D–F). The mutation in the SL-2 loop region that reduced transport also resulted
207 in reduced binding to an RBP in neuronal granules (Fig. 5A). These results indicated that the transport signal
208 may be regulated by the intact sequence of the SL-2 region via the binding to RBPs. Several studies have
209 reported signals of transport and recognition by RBP(s) of some dendritic mRNAs, such as CaMKIIα (26),
210 postsynaptic density protein 95 (PSD-95) (27), and BDNF (28). However, the consensus sequence or motif for
211 mRNA transport has not been elucidated, and the SL-2 sequence does not contain sequences similar to known
212 transport signals. The transport of TBEV genomic RNA reduced the transport of dendritic mRNA, especially

BDNF mRNA (Fig. 6). The genomic RNA of TBEV and dendritic mRNA may share competing RNA sequences or structures required for transport. This information regarding the viral signal element will contribute to further understanding of the transport mechanism of dendritic mRNA which is important for neuronal functions.

RBPs, such as FMRP (14, 29), Staufen (12), and RNG105 (13), are primary components of the neuronal granule and regulate RNA transport and local translation. Our data showed that FMRP interacted with the genomic RNA of TBEV and accumulated at the site of local TBEV replication (Figs. 4, 5, S5 and S6), while Staufen and RNG105 did not. It is possible that this unusual localization of FMRP disrupted the local translation of host dendritic mRNAs bound to FMRP in dendrites, resulting in the development of neurological disease.

The neurological symptoms of TBEV in mice were exacerbated by genome transport and local replication in dendrites. The defect of the transport of the TBEV genomic RNA did not affect the lethality following to viral encephalitis, but was involved in the attenuation of neurological symptoms (Fig. 3). Neurological symptoms caused by the RNA transport might be somehow independent of the lethality by encephalitis. Recent studies have shown that disruption of the transport and local translation of dendritic mRNAs is involved in many neurodegenerative disorders. In fragile X syndrome, mutations and silencing of the *FMRP* gene caused dysregulation of the local translation of the dendritic mRNAs, such as the metabotropic glutamate receptor (mGluR), and CaMKIIα, resulting in abnormalities of morphology and dendritic function (14, 29). BDNF mRNA and its signaling pathway in dendrites has been shown to be involved in Alzheimer's disease (30). In this study, we showed that TBEV infection caused the unusual localization of FMRP in dendrites (Fig. 4) and that TBEV genomic RNA transport reduced the expression and transport of host dendritic mRNAs by neuronal granules (Figs. 6 and S7). It was reported that neuronal RNA granules and FMRP were involved in mRNA stability (31). It is possible that TBEV genomic RNA disturbed binding of FMRP to dendritic mRNAs, and that the unbound RNAs were not transported by neuronal granule, resulting in their degradation. These data indicated that the disturbed transport of host dendritic mRNA by TBEV caused neuronal dysfunction, exacerbating the neurological symptoms in TBEV infected mice. Our

previous report (10) showed that the local replication of TBEV altered the membrane structure in dendrites, suggesting that dendritic degeneration caused by this membrane alteration may also be involved in neuronal dysfunction.

The sequence of the SL-2 region is completely conserved among tick-borne flaviviruses, but not among mosquito-borne viruses (Fig. S8). Our previous study showed that various tick-borne flaviviruses replicate locally in the dendrites (10). In the transmission cycle of tick-borne flaviviruses, ticks get infected through blood suckling of viremic mammals or co-feeding of infected ticks. Viral infection and replication in the central nervous system of mammals are considered non-essential processes for transmission (4). A recent study showed that the UTR sequence that regulates the innate immune system was important for the epidemiological fitness of Dengue virus in a human epidemic (32). It has also been suggested that the tick FMRP ortholog is involved in the tick RNAi pathway (33). Binding of the SL-2 to the tick FMRP or related protein might be important for tick-borne flaviviruses to evade RNAi pathway, resulting in conservation of the sequences.

In this study, we revealed the mechanism of transport of TBEV genomic RNA in neuronal dendrites and demonstrated the involvement of this transport in the development of neurological disease caused by TBEV infection. We propose a model of viral replication and neuronal dysfunction in dendrites caused by TBEV infection (Fig. S9). The genomic RNA of TBEV is transported with RBPs in a neuronal granule. Transport of the viral RNA disturbed that of the host dendritic mRNAs and disrupts the distribution of the components of neuronal granules, such as FMRP. Local replication of the viral genomic RNA in dendrites causes degeneration of the dendrites as shown in our previous study (10). The transport and local replication of the viral RNA may result in neuronal dysfunction leading to the neurological symptoms observed with TBEV infection. To our knowledge, this is the first report showing the hijacking of the neuronal granule system by a neuropathogenic virus for the transport of viral genomic RNA in dendrites. The description of this unique virus-host interaction will improve further understanding of the molecular mechanisms of viral replication and the pathogenicity of neurotropic viruses. It will also promote the study of neurodegenerative diseases caused by disruption of dendritic mRNA transport and could lead to the development of treatment options with

265 virus-based vectors that can transport and express target genes locally in dendrites.

266

267 ## Methods

268 *Localization analysis*

269 Differentiated PC12 cells or primary neuronal cultures of mouse embryo were infected with TBEV or
270 transfected with RNA expression plasmids. The localizations of the RNAs and proteins were analyzed by
271 indirect immunofluorescence assay and FISH.

272

273 *Animal model*

274 C57/BL6 mice were inoculated with 100 plaque forming units of TBEV. Surviving mice were
275 monitored for 14 days, and levels of paralysis and neurological symptoms were evaluated. The President of
276 Hokkaido University approved all animal experiments after review by the Animal Care and Use Committee of
277 Hokkaido University (approval no. 13025).

278

279 *RNA-binding assay*

280 *In-vitro* synthesized RNAs for TBEV genome were mixed with Flag-FMRP expressed in 293T cells.
281 Following immunoprecipitation with anti-Flag antibody, co-precipitated TBEV RNA was detected by
282 RT-PCR.

283

284 Method details were descripted in supplemental methods.

285

286 ## Acknowledgements

287 We would like to thank Dr. T. Igarashi (Kyoto University, Kyoto, Japan) and Dr. N. Shiina (National
288 Institute for Basic Biology, Okazaki, Japan) for kindly providing us the plasmid expressing TBEV replicon
289 RNA and providing us the antibodies against RNG105, respectively. We are grateful to Ms. M. Ishizuka for
290 technical assistance in the experiments.

291 This work is supported by by Grants-in-Aid for Scientific Research (24780293, 25304040, 25304040,
292 26660220, 15J00686, 15K19069, 16J00854 and 16K15032) from the Ministry of Education, Culture, Sports,
293 Sciences and Technology of Japan, The Research Program on Emerging and Re-emerging Infectious Diseases

from Japan Agency for Medical Research and development, AMED, Grants-in-Aid for Regional R&D Proposal-Based Program from Northern Advancement Center for Science & Technology of Hokkaido Japan, Grants-in-Aid for Medical Research from Takeda Science Foundation, and the grand provided by The Ichiro Kanehara Foundation. M. H. and M.M. were supported by a JSPS Grant for Young Scientists.

References

1. Lindenbach BD, Rice CM (2007) Flaviviridae: The Viruses and Their Replication. *Fields Virol*:1101–1151.

2. Friedrich S, et al. (2014) AUF1 p45 Promotes West Nile Virus Replication by an RNA Chaperone Activity That Supports Cyclization of the Viral Genome. *J Virol* 88(19):11586–11599.

3. Liu Z-Y, et al. (2016) Viral RNA switch mediates the dynamic control of flavivirus replicase recruitment by genome cyclization. *Elife* 5:39926–39937.

4. Gould E, Solomon T (2008) Pathogenic flaviviruses. *Lancet* 371(9611):500–509.

5. Zanluca C, et al. (2015) First report of autochthonous transmission of Zika virus in Brazil. *Mem Inst Oswaldo Cruz* 110(4):569–72.

6. Grobbelaar AA, et al. (2016) Resurgence of Yellow Fever in Angola, 2015-2016. *Emerg Infect Dis* 22(10):1854–5.

7. Nagata N, et al. (2015) The Pathogenesis of 3 Neurotropic Flaviviruses in a Mouse Model Depends on the Route of Neuroinvasion After Viremia. *J Neuropathol Exp Neurol* 74(3).

8. Czupryna P, et al. (2011) Tick-borne encephalitis in Poland in years 1993-2008 - epidemiology and clinical presentation. A retrospective study of 687 patients. *Eur J Neurol* 18(5):673–679.

9. Mickiene A, et al. (2002) Tickborne encephalitis in an area of high endemicity in lithuania: disease severity and long-term prognosis. *Clin Infect Dis* 35(6):650–8.

10. Hirano M, et al. (2014) Tick-borne flaviviruses alter membrane structure and replicate in dendrites of primary mouse neuronal cultures. *J Gen Virol* 95(Pt_4):849–861.

11. Doyle M, Kiebler MA (2011) Mechanisms of dendritic mRNA transport and its role in synaptic tagging. *EMBO J* 30(17):3540–52.

12. Lebeau G, et al. (2008) Staufen1 regulation of protein synthesis-dependent long-term potentiation and synaptic function in hippocampal pyramidal cells. *Mol Cell Biol* 28(9):2896–907.

13. Shiina N, Yamaguchi K, Tokunaga M (2010) RNG105 Deficiency Impairs the Dendritic Localization of mRNAs for Na+/K+ ATPase Subunit Isoforms and Leads to the Degeneration of Neuronal Networks. *J Neurosci* 30(38):12816–12830.

14. Kao D-I, Aldridge GM, Weiler IJ, Greenough WT (2010) Altered mRNA transport, docking, and protein translation in neurons lacking fragile X mental retardation protein. *Proc Natl Acad Sci* 107(35):15601–15606.

15. Ohashi R, et al. (2016) Comprehensive behavioral analysis of RNG105 (Caprin1) heterozygous mice: Reduced social interaction and attenuated response to novelty. *Sci Rep* 6:20775.

16. Mus E, Hof PR, Tiedge H (2007) Dendritic BC200 RNA in aging and in Alzheimer's disease. *Proc Natl Acad Sci* 104(25):10679–10684.

17. Bílý T, et al. (2015) Electron Tomography Analysis of Tick-Borne Encephalitis Virus Infection in Human Neurons. *Sci Rep* 5:10745.

18. Kofler RM, Hoenninger VM, Thurner C, Mandl CW (2006) Functional analysis of the tick-borne encephalitis virus cyclization elements indicates major differences between mosquito-borne and tick-borne flaviviruses. *J Virol* 80(8):4099–113.

19. Schrier M, et al. (2004) Transport kinetics of FMRP containing the I304N mutation of severe fragile X syndrome in neurites of living rat PC12 cells. *Exp Neurol* 189(2):343–353.

20. Ascano M, et al. (2012) FMRP targets distinct mRNA sequence elements to regulate protein expression. *Nature* 492(7429):382–386.

21. Salinas S, Schiavo G, Kremer EJ (2010) A hitchhiker's guide to the nervous system: the complex journey of viruses and toxins. *Nat Rev Microbiol* 8(9):645–655.

22. Owen D, Crump C, Graham S (2015) Tegument Assembly and Secondary Envelopment of Alphaherpesviruses. *Viruses* 7(9):5084–5114.

23. Ohka S, et al. (2009) Receptor-dependent and -independent axonal retrograde transport of poliovirus in motor neurons. *J Virol* 83(10):4995–5004.

24. Klingen Y, Conzelmann K-K, Finke S (2008) Double-labeled rabies virus: live tracking of enveloped virus transport. *J Virol* 82(1):237–45.

25. Filomatori C V., et al. (2006) A 5’ RNA element promotes dengue virus RNA synthesis on a circular genome. *Genes Dev* 20(16):2238–2249.

26. Mori Y, Imaizumi K, Katayama T, Yoneda T, Tohyama M (2000) Two cis-acting elements in the 3’ untranslated region of alpha-CaMKII regulate its dendritic targeting. *Nat Neurosci* 3(11):1079–84.

27. Subramanian M, et al. (2011) G-quadruplex RNA structure as a signal for neurite mRNA targeting. *EMBO Rep* 12(7):697–704.

28. Chiaruttini C, et al. (2009) Dendritic trafficking of BDNF mRNA is mediated by translin and blocked by the G196A (Val66Met) mutation. *Proc Natl Acad Sci U S A* 106(38):16481–6.

29. Dictenberg JB, Swanger SA, Antar LN, Singer RH, Bassell GJ (2008) A Direct Role for FMRP in Activity-Dependent Dendritic mRNA Transport Links Filopodial-Spine Morphogenesis to Fragile X Syndrome. *Dev Cell* 14(6):926–939.

30. Tapia-Arancibia L, Aliaga E, Silhol M, Arancibia S (2008) New insights into brain BDNF function in normal aging and Alzheimer disease. *Brain Res Rev* 59(1):201–220.

31. De Rubeis S, Bagni C (2010) Fragile X mental retardation protein control of neuronal mRNA metabolism: Insights into mRNA stability. *Mol Cell Neurosci* 43(1):43–50.

32. Manokaran G, et al. (2015) Dengue subgenomic RNA binds TRIM25 to inhibit interferon expression for epidemiological fitness. *Science (80-)* 350(6257).

33. Kurscheid S, et al. (2009) Evidence of a tick RNAi pathway by comparative genomics and reverse genetics screen of targets with known loss-of-function phenotypes in Drosophila. *BMC Mol Biol* 10(1):26.

34. Viesselmann C, Ballweg J, Lumbard D, Dent EW (2011) Nucleofection and Primary Culture of Embryonic Mouse Hippocampal and Cortical Neurons. *J Vis Exp* (47). doi:10.3791/2373.

35. Takashima I, et al. (1997) A case of tick-borne encephalitis in Japan and isolation of the the virus. *J Clin Microbiol* 35(8):1943–7.

36. Takano A, et al. (2011) Construction of a replicon and an infectious cDNA clone of the Sofjin strain of the Far-Eastern subtype of tick-borne encephalitis virus. *Arch Virol* 156(11):1931–1941.

37. Phongphaew W, et al. (2017) Valosin-containing protein (VCP/p97) plays a role in the replication of West Nile virus. *Virus Res* 228:114–123.

375 38. Yoshii, K., Konno A, Goto A, Nio J, Obara M, Ueki T, Hayasaka D, Mizutani T, Kariwa H TI (2004) Single
376 point mutation in tick-borne encephalitis virus prM protein induces a reduction of virus particle secretion. *J Gen*
377 *Virol* 85(10):3049–3058.

378 39. Schneider CA, Rasband WS, Eliceiri KW (2012) NIH Image to ImageJ: 25 years of image analysis. *Nat Methods*
379 9(7):671–675.

380 40. Guyenet SJ, et al. (2010) A Simple Composite Phenotype Scoring System for Evaluating Mouse Models of
381 Cerebellar Ataxia. *J Vis Exp* (39):e1787–e1787.

382 41. Zuker M (2003) Mfold web server for nucleic acid folding and hybridization prediction. *Nucleic Acids Res*
383 31(13):3406–15.

384

385 **Figure Legends**

386 **Figure 1. 5' untranslated region (UTR) of tick-borne encephalitis virus (TBEV) functions as a**
387 **signal of RNA transport to the neurites of PC12 cells.**

388 Differentiated PC12 cells were transfected with the plasmids expressing the RNA of luciferase with TBEV
389 sequences (A-C) or with TBEV/West Nile virus (WNV) UTRs (D−F). Following fixation, the cells were
390 hybridized with a fluorescent RNA probe for the *luciferase* gene (green), and stained with DAPI (blue) and
391 antibodies against microtubule-associated protein 2 (MAP2; magenta). Fluorescent in-situ hybridization
392 (FISH) signal in the neurites was analyzed from the Z-stack images from five independent microscopic fields.
393 (A) A coding sequence (CDS) for *luciferase* (gray square) was cloned with or without the partial sequence for
394 TBEV replicon RNA. (B, E) Fluorescence images and (C, F) fluorescence intensity in the PC12 neurites. (D)
395 A CDS for luciferase was cloned with/without the 5' and 3' UTRs of TBEV (black line) and WNV (striped
396 line). Scale bars indicate 5 μm in length. White arrows indicate the FISH signal for luciferase RNA in the
397 neurites. Error bars represent standard error (SEM); $^{**}p < 0.02$ and $^{*}p < 0.05$.

398

399 **Figure 2. Analysis of the roles of the stem-loop structure of TBEV 5' UTR in genome transport.**

400 Differentiated PC12 cells were transfected with the plasmids expressing the mRNA of luciferase with the
401 UTRs of TBEV with deletion (A−C) or the mutation (D−F) of 5' UTR. Following fixation, the cells were
402 hybridized with a fluorescent RNA probe for the *luciferase* gene (green), and stained with DAPI (blue) and
403 antibodies against MAP2 protein (magenta). FISH signal in the neurites was analyzed from the Z-stack
404 images from five independent microscopic fields. (A) Schematic diagram of the predicted RNA-secondary
405 structure (upper) and the constructs expressing mRNA with a deletion (lower) are shown. The 5' UTR has a
406 predicted branched stem loop (SL-) structures (SL-1) and single SL-structure (SL-2). The SL-1 or the SL-2

regions were deleted in pCMV-Luc (5' TBEV/3' TBEV). (B, E) Fluorescence images and (C, F) fluorescence intensity in the PC12 neurites. (D) Schematic diagram of the sequence and RNA secondary structure of the TBEV SL-2 and the constructs used to analyze the role of SL-2 in transport. G-to-U, C-to-U in loop, or four mutations in stem were introduced in pCMV (5' TBEV/3' TBEV). Scale bars indicate 5 μm in length. White arrows indicate the FISH signal for luciferase RNA in the neurites. Error bars represent SEM; $**p < 0.02$ and $*p < 0.05$.

Figure 3. Mutation impeding genome transport to dendrites attenuated the neurological symptoms caused by TBEV infection.

(A, B) Primary mouse neurons were infected with TBEV wild-type (wt; black squares with continuous lines) or SL-2 loop C-U (white circles with broken lines) at a multiplicity of infection (MOI) of 0.1. (A) The cells were fixed at 48 h.p.i. and the viral proteins and viral genomic RNAs were stained with IFA (upper panels, magenta) and FISH (lower panels, green), respectively. (B) Viral antigen accumulation was counted at 24, 48, or 72 h.p.i. in five independent microscopic fields. White scale bars indicate 5 μm in length. White arrows indicate viral antigen accumulation or the viral genome in dendrites. (C−E) Five-week-old male C57BL/6 mice were inoculated with 100 plaque forming units of TBEV wt or SL-2 loop C-U intracerebrally. (C) The Kaplan−Meier survival estimate was calculated ($n = 10$). (D) The neurological score of the mice ($n = 5$) was examined until 8 d post-infection (d.p.i.). (E) The mice were sacrificed at 3 or 6 d.p.i. ($n = 3$), and the viral titer in the brain were analyzed. Continuous and broken lines indicate the average of viral titer in the brain infected with TBEV wt and SL-2 loop C-U, respectively. Error bars represent SEM; $**p < 0.02$ and $*p < 0.05$.

Figure 4. Localization of the RNA-binding proteins (RBPs) of neuronal granule in neuron infected with TBEV.

Primary mouse neurons were uninfected or infected with TBEV wt or SL-2 loop C-U at an MOI of 0.1. The cells were fixed at 48 h.p.i and stained with antibodies against fragile X mental retardation protein (FMRP), RNA granule protein 105 (RNG105), or Staufen (green), and antibodies against viral proteins (magenta). (A) Fluorescent images of the neurons. (B) The signals of RBPs in the cell body or neurites were analyzed in Z-Stack images of five microscopic fields. Error bars represent SEM; $**p < 0.02$ and $*p < 0.05$.

Figure 5. Interaction between the RBP of a neuronal granule and the genomic RNA of TBEV.

Full-length RNAs of TBEV wt (wt) or of SL-2 loop C-U (C-U) (A) was mixed with cell lysate expressing Flag-FMRP wt (wt) or I304N (B). The mixture was immuneprecipitated (IP) with beads with anti-Flag antibody (Flag) or beads only (Control), and precipitated protein and RNA were detected by Western blotting

(WB) and reverse transcription (RT-) PCR, respectively. Right panels show expression of the FMRP wt or I304N in total cell lysate.

Figure 6. TBEV infection and transport of viral RNA disrupted the localization of dendritic mRNAs.

Primary mouse neurons were infected with TBEV wt or SL-2 loop C-U at an MOI of 0.1. (A) The cells were fixed at 48 h.p.i. and mRNA for Arc, brain-derived neurotropic factor (BDNF), or Ca^{2+}/calmodulin-dependent protein kinase II α (CaMKIIα) was stained by FISH (green). Scale bars indicate 5 μm in length. (B) Fluorescent signal of the mRNA for Arc, BDNF, or CaMKIIα in dendrites were measured in ten areas of interest (AOI). Error bars represent SEM; $^{**}p < 0.02$ and $^{*}p < 0.05$.

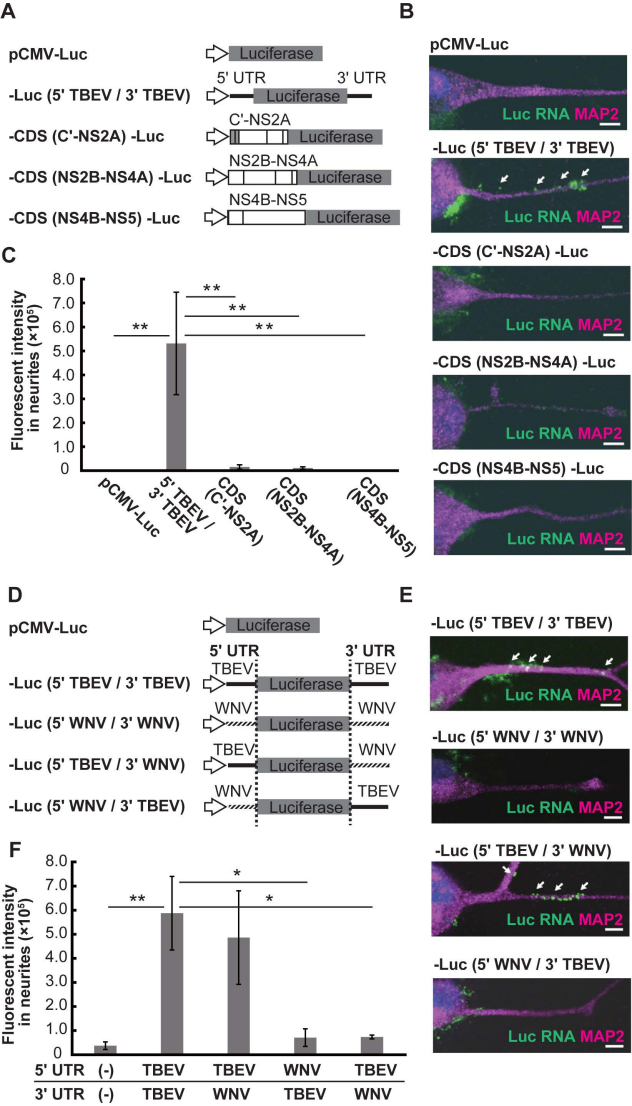
A
pCMV-Luc
Luciferase
-Luc (5' TBEV / 3' TBEV)
5' UTR
3' UTR
Luciferase
-CDS (C'-NS2A) -Luc
C'-NS2A
Luciferase
-CDS (NS2B-NS4A) -Luc
NS2B-NS4A
Luciferase
-CDS (NS4B-NS5) -Luc
NS4B-NS5
Luciferase
B
pCMV-Luc
Luc RNA MAP2
-Luc (5' TBEV / 3' TBEV)
Luc RNA MAP2
-CDS (C'-NS2A) -Luc
Luc RNA MAP2
-CDS (NS2B-NS4A) -Luc
Luc RNA MAP2
-CDS (NS4B-NS5) -Luc
Luc RNA MAP2
C
Fluorescent intensity in neurites (×10⁵)
8.0
7.0
6.0
5.0
4.0
3.0
2.0
1.0
0
**
**
**
**
pCMV-Luc
5' TBEV / 3' TBEV
CDS (C'-NS2A)
CDS (NS2B-NS4A)
CDS (NS4B-NS5)
D
pCMV-Luc
Luciferase
5' UTR
3' UTR
-Luc (5' TBEV / 3' TBEV)
TBEV
TBEV
Luciferase
-Luc (5' WNV / 3' WNV)
WNV
WNV
Luciferase
-Luc (5' TBEV / 3' WNV)
TBEV
WNV
Luciferase
-Luc (5' WNV / 3' TBEV)
WNV
TBEV
Luciferase
E
-Luc (5' TBEV / 3' TBEV)
Luc RNA MAP2
-Luc (5' WNV / 3' WNV)
Luc RNA MAP2
-Luc (5' TBEV / 3' WNV)
Luc RNA MAP2
-Luc (5' WNV / 3' TBEV)
Luc RNA MAP2
F
Fluorescent intensity in neurites (×10⁵)
8.0
7.0
6.0
5.0
4.0
3.0
2.0
1.0
0
**
*
*
5' UTR (-) TBEV TBEV WNV TBEV
3' UTR (-) TBEV WNV TBEV WNV

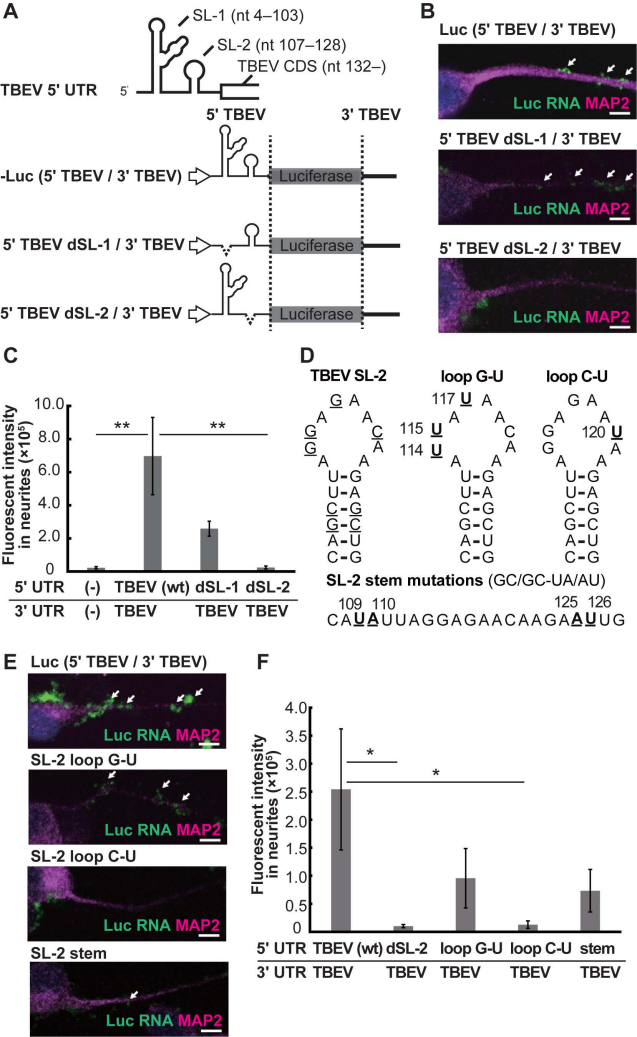
A
SL-1 (nt 4–103)
SL-2 (nt 107–128)
TBEV CDS (nt 132–)
TBEV 5' UTR
5'
5' TBEV
3' TBEV
-Luc (5' TBEV / 3' TBEV)
Luciferase
5' TBEV dSL-1 / 3' TBEV
Luciferase
5' TBEV dSL-2 / 3' TBEV
Luciferase
B
Luc (5' TBEV / 3' TBEV)
Luc RNA MAP2
5' TBEV dSL-1 / 3' TBEV
Luc RNA MAP2
5' TBEV dSL-2 / 3' TBEV
Luc RNA MAP2
C
Fluorescent intensity in neurites (×10⁵)
10.0
8.0
6.0
4.0
2.0
0
**
**
5' UTR (-) TBEV (wt) dSL-1 dSL-2
3' UTR (-) TBEV TBEV TBEV
D
TBEV SL-2
loop G-U
loop C-U
117 U
115 U
114 U
120 U
U-G
U-A
C-G
G-C
A-U
C-G
SL-2 stem mutations (GC/GC-UA/AU)
109 110
CAUAUUAGGAGAACAAGAAUUG
125 126
E
Luc (5' TBEV / 3' TBEV)
Luc RNA MAP2
SL-2 loop G-U
Luc RNA MAP2
SL-2 loop C-U
Luc RNA MAP2
SL-2 stem
Luc RNA MAP2
F
Fluorescent intensity in neurites (×10⁵)
4.0
3.5
3.0
2.5
2.0
1.5
1.0
0.5
0
*
*
5' UTR TBEV (wt) dSL-2 loop G-U loop C-U stem
3' UTR TBEV TBEV TBEV TBEV TBEV

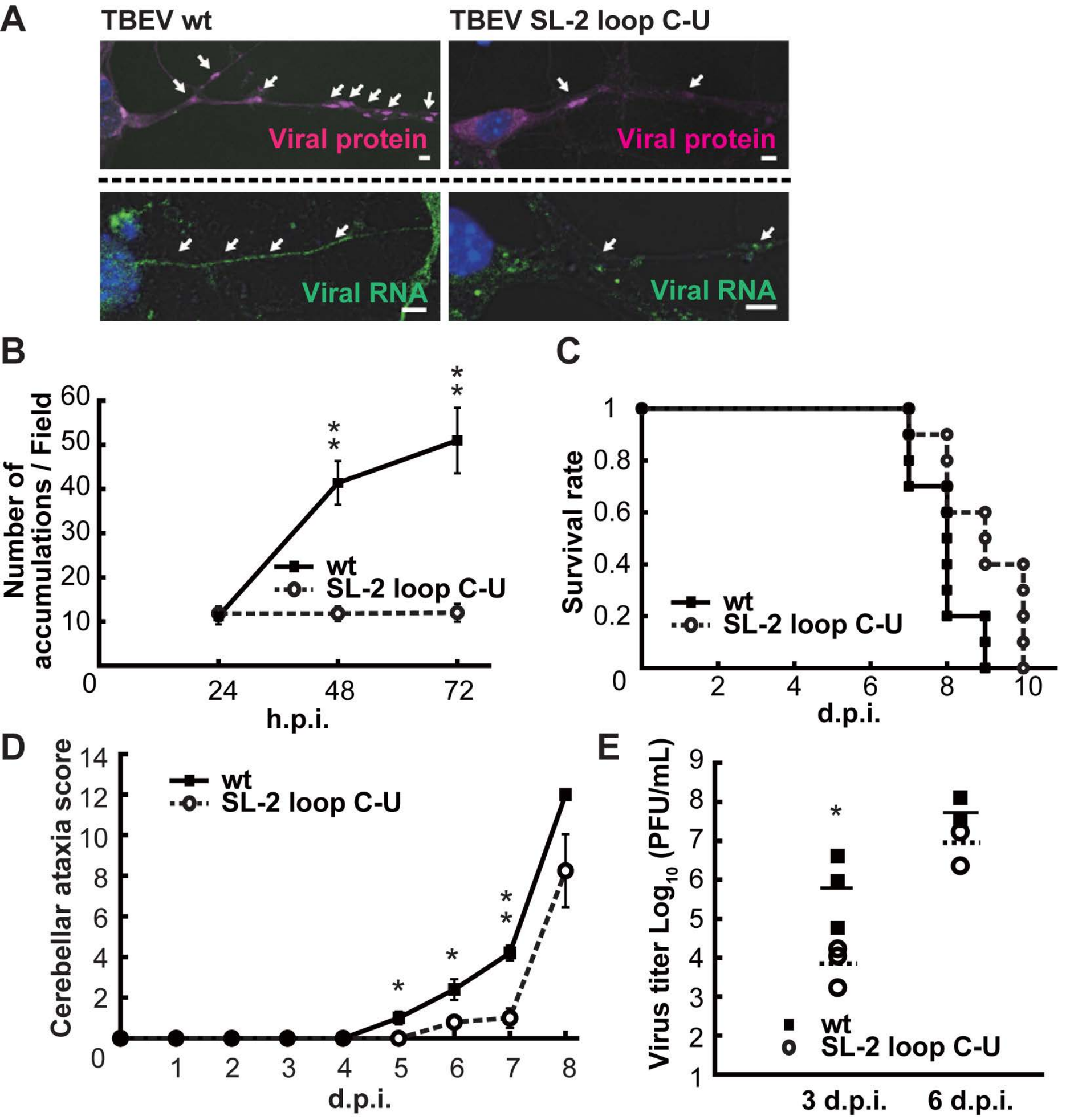
A
TBEV wt
TBEV SL-2 loop C-U
Viral protein
Viral protein
Viral RNA
Viral RNA
B
Number of accumulations / Field
60
50
40
30
20
10
0
24
48
72
h.p.i.
wt
SL-2 loop C-U
**
**
C
Survival rate
1
0.8
0.6
0.4
0.2
0
2
4
6
8
10
d.p.i.
wt
SL-2 loop C-U
D
Cerebellar ataxia score
14
12
10
8
6
4
2
0
1
2
3
4
5
6
7
8
d.p.i.
wt
SL-2 loop C-U
*
*
**
E
Virus titer Log10 (PFU/mL)
9
8
7
6
5
4
3
2
1
*
wt
SL-2 loop C-U
3 d.p.i.
6 d.p.i.

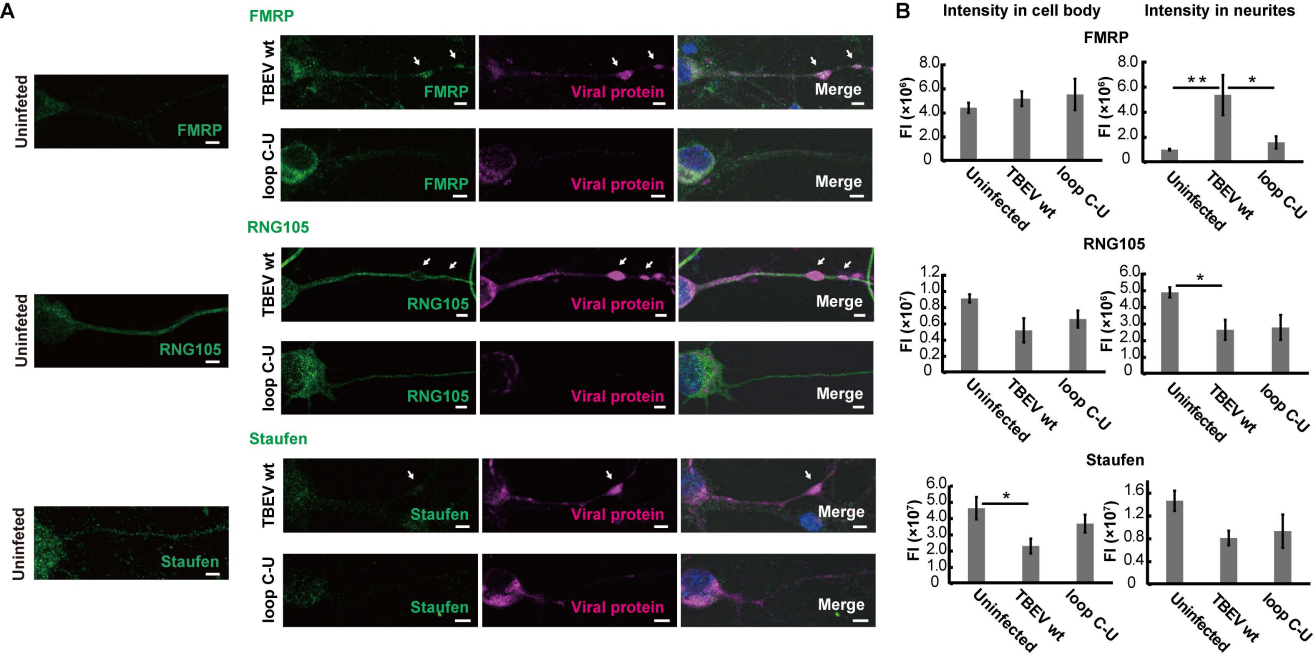
A
FMRP
Uninfeted
FMRP
TBEV wt
FMRP
Viral protein
Merge
loop C-U
FMRP
Viral protein
Merge
RNG105
Uninfeted
RNG105
TBEV wt
RNG105
Viral protein
Merge
loop C-U
RNG105
Viral protein
Merge
Staufen
Uninfeted
Staufen
TBEV wt
Staufen
Viral protein
Merge
loop C-U
Staufen
Viral protein
Merge
B
Intensity in cell body
Intensity in neurites
FMRP
FI (×10⁶)
8.0
6.0
4.0
2.0
0
Uninfected
TBEV wt
loop C-U
**
*
RNG105
FI (×10⁷)
1.2
1.0
0.8
0.6
0.4
0.2
FI (×10⁶)
6.0
5.0
4.0
3.0
2.0
1.0
Staufen
FI (×10⁷)
1.6
1.2
0.8
0.4

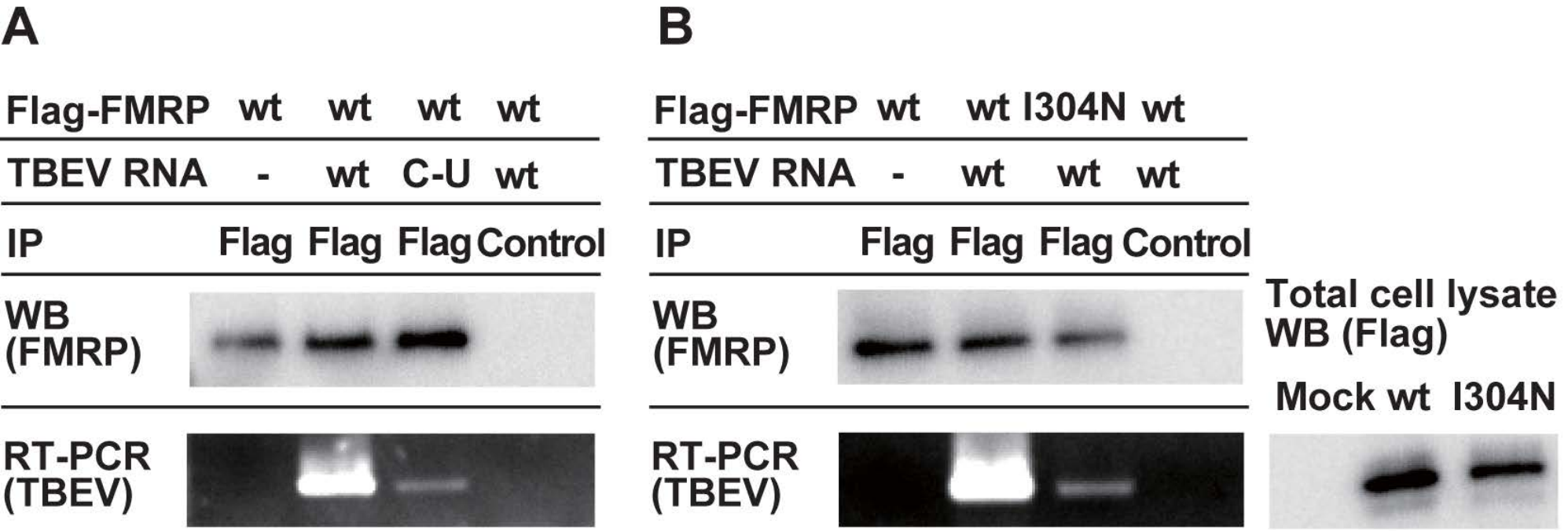
A
Flag-FMRP wt wt wt wt
TBEV RNA - wt C-U wt
IP Flag Flag Flag Control
WB (FMRP)
RT-PCR (TBEV)
B
Flag-FMRP wt wt I304N wt
TBEV RNA - wt wt wt
IP Flag Flag Flag Control
WB (FMRP)
RT-PCR (TBEV)
Total cell lysate WB (Flag)
Mock wt I304N

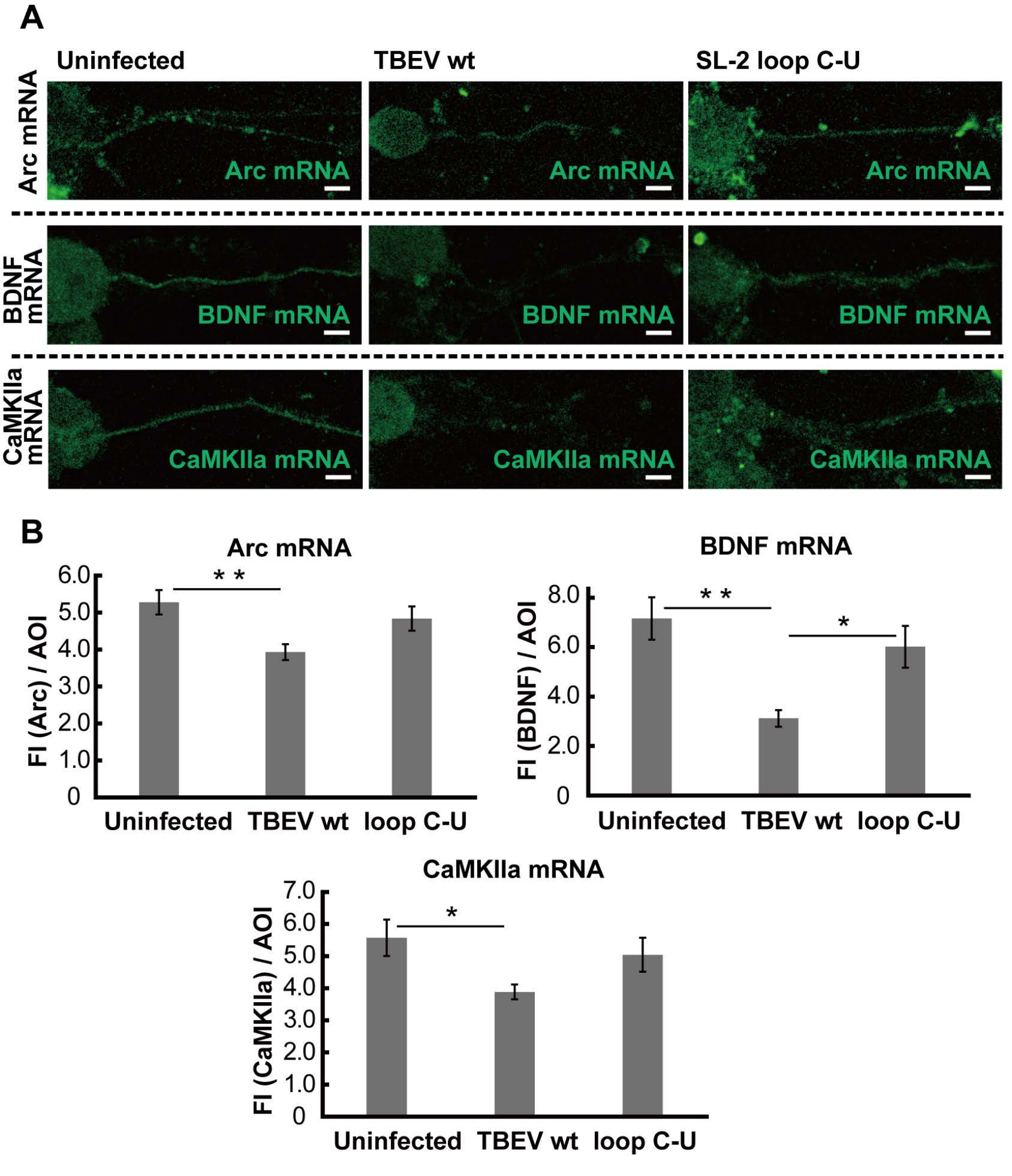
A
Uninfected
TBEV wt
SL-2 loop C-U
Arc mRNA
Arc mRNA
Arc mRNA
Arc mRNA
BDNF mRNA
BDNF mRNA
BDNF mRNA
BDNF mRNA
CaMKIIa mRNA
CaMKIIa mRNA
CaMKIIa mRNA
CaMKIIa mRNA
B
Arc mRNA
FI (Arc) / AOI
6.0
5.0
4.0
3.0
2.0
1.0
0
* *
Uninfected
TBEV wt
loop C-U
BDNF mRNA
FI (BDNF) / AOI
8.0
6.0
4.0
2.0
0
* *
*
Uninfected
TBEV wt
loop C-U
CaMKIIa mRNA
FI (CaMKIIa) / AOI
7.0
6.0
5.0
4.0
3.0
2.0
1.0
0
*
Uninfected
TBEV wt
loop C-U